Radical Ions of α,α′-Bis(diphenylamino)-capped Oligothiophenes: A Combined Spectroelectrochemical and Theoretical Study

Dirk Rohde,[†] Lothar Dunsch,[†] Ahacine Tabet,[‡] Horst Hartmann,*[,‡] and Jürgen Fabian[‡]

Leibniz-Institut für Festkörper- und Werkstoffforschung, Abteilung Elektrochemie und Leitfähige Polymere, Helmholtzstrasse 20, D-01069 Dresden, Germany, and Institut für Organische Chemie, Technische Universität, Mommsenstrasse 6, D-01069 Dresden, Germany

Received: August 7, 2005; In Final Form: January 25, 2006

A new homologous series of α,α′-bis(diphenylamino)-capped oligothiophenes, prepared by a palladium-catalyzed coupling reaction of stannylated 2-diphenylaminothiophenes with 2-mono- or 2,5-dibromothiophenes and their homologues, was studied by in situ ESR/UV−vis/NIR spectroelectrochemistry. In general, the oxidation potentials of these oligothiophenes were found to be proportional to the inverse number of thiophene units. However, the potential slope of the first oxidation is completely different from that of higher oxidation steps. Trication radicals were identified by electron spin resonance (ESR) for higher thiophene homologues in addition to monocation radicals (polarons). According to the ESR hyperfine structures, the unpaired electron is delocalized in the conjugated system. In contrast to the parent α,α′-bis(diphenylamino)-capped oligothiophenes, the UV−vis/NIR absorption maxima of the oxidized species strongly depend on the number of thiophene units. Spin-restricted and spin-unrestricted Kohn−Sham density functional calculations were used to explain and to understand these properties. Absorption wavelength and intensities were calculated by the time-dependent density functional response theory. Unrestricted density functional calculations of oligothiophene dications (bipolarons) with five or more thiophene rings result in spin-broken structures which may be considered as two-polaron biradicals (polaron pairs).

Introduction

Recently, *N*-perarylated aromatic amines, diamines, and triamines, such as compounds **1**−**3**, received strong interest in both synthetic and structural studies. They usually form, after cooling their melts, amorphous glasses which results in a high stability and pronounced mobility of the positively charged species generated by oxidation.[1] Thus, these compounds exhibit a remarkable electrical conductivity and can be used, therefore, as hole-transport materials for several types of optical and microelectronic devices, such as organic-field-effect transistors,[2] organic light emitting diodes,[3] solar cells,[4] or laser printers and copiers.[5]

Several thiophene derivatives with the *N*-perarylated amine moieties such as compounds **4**−**6**[6] have already been prepared. Similar to their carbocyclic analogues **1** and **2**, they form amorphous glasses and stabilize oxidized species to such an extent that they can be used as materials for hole-transport.[7] To gain more insight into the relationship between the chemical structure and physical properties of the diarylamino- and bis-(diarylamino)-substituted thiophene derivatives **4**−**6**, we have prepared the α-diphenylamino- and α,α′-bis-diphenylamino-substituted compounds (Ar^1/Ar^2 = phenyl) as well as a homologous series of their oligomers of the general structure $\mathbf{10}_n$ and studied their properties in detail by electrochemical and spectroscopic methods.

Although the synthetic routes to these structures have been published recently,[8] a short description of their synthesis is given here. Until recently, only a few *N*,*N*-diaryl-substituted 2-aminothiophenes such as **4**−**6** and some of their homologues were described.[6c,6d] They have been prepared either by simple heterocyclization by one of the authors[6b] or by heavy metal-catalyzed C,C- or C,N-coupling reactions well established in recent years by several authors.[9] Consequently, the α,α′-bis-(diphenylamino)-capped oligothiophenes $\mathbf{10}_n$ have been prepared by three different routes outlined in Scheme 2. In a first route, diphenylamine **7** was coupled with 2-bromothiophene $\mathbf{11}_1$ or 2,5-dibromothiophene $\mathbf{12}_1$ as well as with their higher homologues $\mathbf{11}_2$, $\mathbf{11}_3$, $\mathbf{12}_2$, or $\mathbf{12}_3$ in the presence of $Pd(PPh_3)_2Cl_2$ or $Pd(PPh_3)_4$ as the catalyst. Thus, the diphenylamino-substituted compounds $\mathbf{8}_1$−$\mathbf{8}_3$ as well as the bis(diphenylamino)-substituted compounds $\mathbf{10}_1$−$\mathbf{10}_3$, respectively, have been obtained.[6c]

Due to the lower solubility of the mono- or dibromo compounds $\mathbf{11}_m$ and $\mathbf{12}_m$ with $m > 3$ in organic solvents, the reaction could not effectively extend upon the synthesis of higher homologues of the α-diphenylamino- and α,α′-bis(diphenylamino)-substituted oligothiophenes. Therefore, the 2-diphenyl-

SCHEME 1

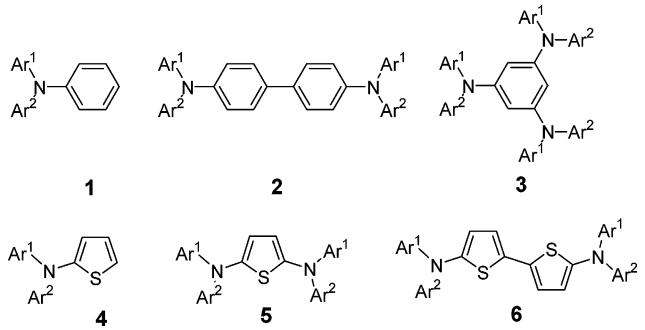

[†] Leibniz-Institut für Festkörper- und Werkstoffforschung (IFW).
[‡] Technische Universität Dresden.
* To whom correspondence should be addressed. Tel: ++49-351 4633 9484. Fax: ++49-351 4633 9486. E-mail: Hartmann@iapp.de.

10.1021/jp054401i CCC: $33.50
Published on Web 04/04/2006

SCHEME 2

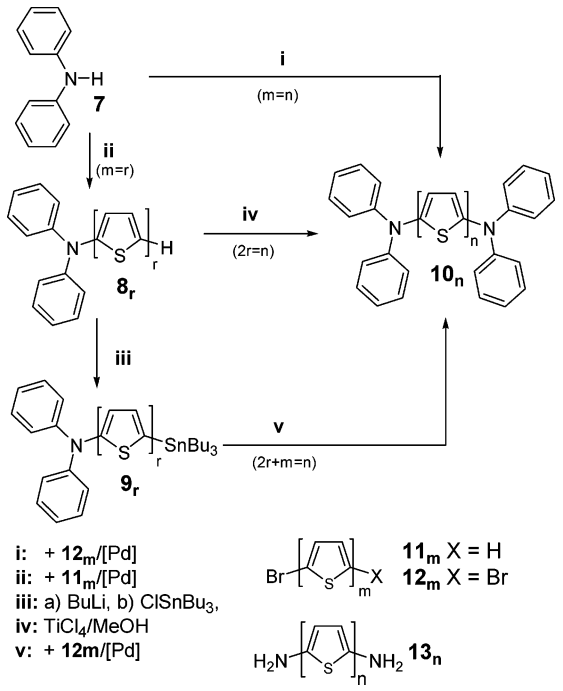

aminothiophenes $\mathbf{8}_1-\mathbf{8}_3$ have been used as parent compounds. These compounds were transformed, at first, into their tributylstannylated derivatives $\mathbf{9}_1-\mathbf{9}_3$ which subsequently react with bromothiophenes $\mathbf{11}_2$ and $\mathbf{11}_3$ or with dibromothiophenes $\mathbf{12}_1-\mathbf{12}_3$ in the presence of the palladium catalysts mentioned above. Thus, the higher homologues of the series $\mathbf{8}_r$ with $r = 2-5$ and $\mathbf{10}_n$ with $n = 3-9$, respectively, have been obtained.[10]

As a third synthesis method for some of the α,α′-bis-(diphenylamino)-substituted oligothiophenes $\mathbf{10}_n$ ($n = 2, 4$), the oxidative dimerization of the 2-diphenylamino-substituted thiophenes $\mathbf{8}_r$ with $r = 1, 2$ by the addition of bromine or iodine and the subsequent addition of $NaBH_4$ or, alternatively, by the addition of titanium tetrachloride has been used.[6e] This procedure was previously applied to the synthesis of *N*,*N*′-persubstituted benzidines from *N*-disubstituted anilines with satisfactory yields.[11]

Similar to their carbocyclic aniline analogues,[12] the α-diphenylamino- and α,α′-bis(diphenylamino)-substituted oligothiophenes $\mathbf{8}_r$ and $\mathbf{10}_n$ were found to be strongly electron-donating compounds. Their redox behavior was measured by cyclic voltammetry in benzonitrile solution containing 0.1 M tetrabutylammonium hexafluorophosphate at a scan rate of 100 mV/s.

Experimental and Computational Methods

The cyclic voltammograms (CVs) were obtained in a three-electrode system at a platinum working as well as counter electrode using a Princeton Applied Research (PAR 270) electrochemical system. A silver wire served as the pseudo-reference electrode. The CV measurements were carried out in a glovebox. Ferrocene was used as an internal potential marker.

Laminated platinum mesh or Gold-LIGA electrodes were used as the working electrode in spectroelectrochemical experiments. In simultaneous ESR and UV−vis/NIR measurements, the structures generated were studied in 0.1 M $TBABF_4$ (Fluka, assay >99%, and dried in a vacuum) solutions of purified and dried benzonitrile (Fluka, assay >99.5%). A silver wire served as the pseudo-reference electrode, and a platinum wire served as the counter electrode as well. ESR spectra were recorded by the X-band spectrometer ELEXYS (Bruker, Germany) and optical spectra by the UV−vis/NIR system TIDAS (J&M, Aalen, Germany). A PG 284 potentiostat/galvanostat (HEKA Electronic, Lambrecht, Germany) was used for electrode potential control in the spectroelectrochemical studies.

Because of the size of the α,α′-bis(diphenylamino)-substituted oligothiophenes, the compounds had to be calculated by methods of the Kohn−Sham density functional theory (DFT)[13] rather than by those of ab initio theory. The calculations were performed with the GAUSSIAN 98 programs.[14] The hybrid HF/DFT method was used with Becke's three-parameter exchange functional (B3)[15] combined with the Lee−Yang−Parr (LYP) correlation functional.[16,17] Open-shell systems were calculated by the spin-unrestricted DFT (UDFT) method.[13] To treat the entire homologous series of compounds consistently, Pople's small valence double-ζ basis set 3-21G was used in general and more extended basis sets were used in selected cases. The effect of solvent was estimated by the self-consistent reaction field method employing the isodensity surface polarized continuum model (IPCM).[18] The experimental conditions in solution were simulated for acetonitrile ($\epsilon = 36.64$ D). To destroy the α,β-spin symmetry, the Guess = Mix option was used. Hyperfine splitting constants were calculated by B3LYP/6-31G* single-point calculations and electronic transition energies by time-dependent DFT (TD-DFT)[13] using the 3-21G or 3-21+G* basis sets. Semiempirical PPP-CIS calculations of spectral data take 225 singly excited configurations (15×15) into account.[19] Electron repulsion was considered by the Mataga−Nishimoto relationship. The PPP calculations were based on DFT geometries using the PPP standard parametrization derived earlier.[20] The distortion of the terminal groups was considered by the cosines of the averaged distortion angles of the amino substituents and of the attached phenyl groups while bond parameters (resonance integrals) were held constant as in former PPP studies. PPP-CIS calculations were carried out with the program WINPPP.[21] Singly occupied molecular orbitals (SOMOs) of the DFT calculations were visualized by MOLDEN.[22]

Results and Discussion

The cyclic voltammograms of α-diphenylamino-substituted oligothiophenes $\mathbf{8}_1$ and $\mathbf{8}_3$ and of α,α′-bis(diphenylamino)-substituted oligothiophenes $\mathbf{10}_1$ and $\mathbf{10}_3$ are given in Figure 1 while the numeric data of the electrochemical measurements of the compounds $\mathbf{8}_r$ with $r = 1-5$ and the compounds $\mathbf{10}_n$ with $n = 1-9$ are compiled in Table 1.

The electrochemical data reveal an irreversible oxidation of the α-diphenylamino-substituted thiophenes $\mathbf{8}_1$ and $\mathbf{8}_2$ while their homologues $\mathbf{8}_3-\mathbf{8}_5$ and all the α,α′-bis(diphenylamino)-substituted oligothiophenes $\mathbf{10}_n$ show a reversible electron transfer at relatively low electrode potentials.

The cyclic voltammograms of compounds $\mathbf{10}_1$ and $\mathbf{10}_2$ differ from those of compounds $\mathbf{10}_3-\mathbf{10}_9$ in that the first electron transfer of compounds $\mathbf{10}_1$ and $\mathbf{10}_2$ consists of two separate one-electron-transfer steps. All the higher homologues $\mathbf{10}_3-\mathbf{10}_9$ give a first single two-electron-transfer step at low oxidation potentials. This behavior is evident when plotting the first and second oxidation potentials of the compounds $\mathbf{10}_n$ vs the reciprocal number *n* of thiophene units (Figure 2). The dependence of the electrode potential of oligothiophenes $\mathbf{10}_n$ for the first and second oxidation steps vs $1/n$ gives an intersect at $1/n = 0.33$ by extrapolation. Therefore, for the trimer and the higher homologues, the first and second oxidation potentials are overlapped to form a single two-electron step.

Terthiophene $\mathbf{10}_3$ (as well as its higher homologues) undergoes a transfer of up to three electrons in electrochemical

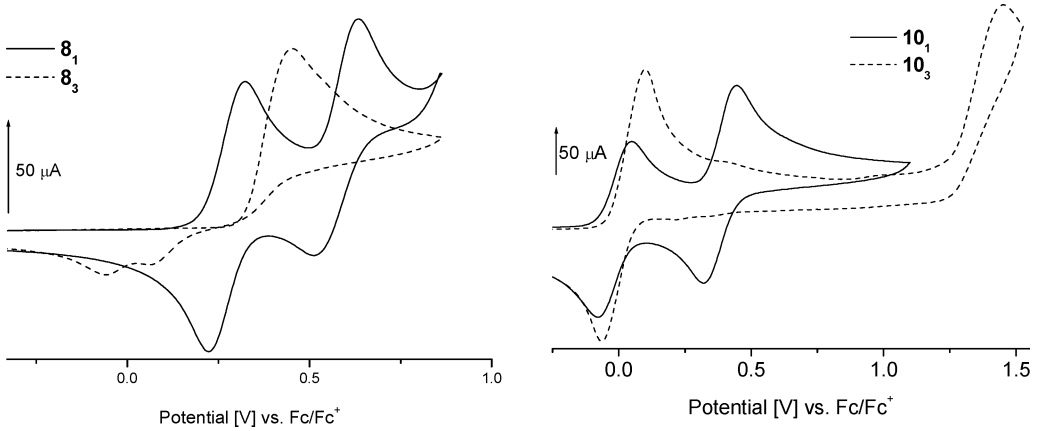

Figure 1. Cyclic voltammograms of compounds $\mathbf{8}_1$, $\mathbf{8}_3$, $\mathbf{10}_1$, and $\mathbf{10}_3$ measured in benzonitrile containing 0.1 M tetrabutylammonium hexafluorophosphate at a scan rate of 100 mV/s using a ferrocene couple as the potential reference.

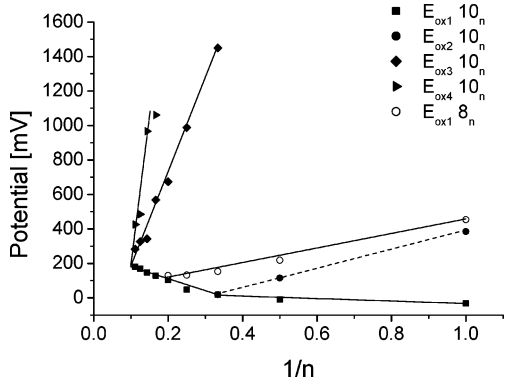

Figure 2. Dependence of the electrochemical oxidation potentials on the reciprocal number *n* of thiophene units.

TABLE 1: Observed Electrochemical Data[a] of Compounds $\mathbf{10}_1-\mathbf{10}_9$ and $\mathbf{8}_1-\mathbf{8}_5$ Measured in Benzonitrile (1×10^{-3} M), Containing 0.1 M Tetrabutylammonium Hexafluorophosphate, Scan Rate 100 nV/s, vs Ferrocene

entry	E_{ox1} (mV)	E_{ox2} (mV)	E_{ox3} (mV)	E_{ox4} (mV)	E_{ox5} (mV)
$\mathbf{10}_1$	-32-1-rev	384-1-rev			
$\mathbf{10}_2$	-10-1-rev	115-1-rev			
$\mathbf{10}_3$	18-2-rev	1450-1-ir			
$\mathbf{10}_4$	48-2-rev	987-1-qrev			
$\mathbf{10}_5$	102-2-qrev	674-1-qrev			
$\mathbf{10}_6$	128-2-rev	567-1-rev		846-1-ir	1060-1-ir
$\mathbf{10}_7$	148-2-rev	342-1-rev		635-1-qrev	966-1-ir
$\mathbf{10}_8$	169-2-rev	326-1-rev		484-1-qrev	877-1-ir
$\mathbf{10}_9$	180-2-rev	283-1-rev		425-1-rev	770-1-ir
$\mathbf{8}_1$	454-1-ir				
$\mathbf{8}_2$	218-1-qrev				
$\mathbf{8}_3$	153-1-rev	470-1-qrev			
$\mathbf{8}_4$	132-1 rev	362-1-rev			
$\mathbf{8}_5$	130-1-rev	283-1-rev	1093-1-ir		

[a] Oxidation potentials in mV−number of electrons−reversibility.

oxidation while pentamer $\mathbf{10}_5$ (and its homologues) transfers up to five electrons. The electron transfers at higher potentials are irreversible. Compounds $\mathbf{10}_6-\mathbf{10}_9$ give a third oxidation step in cyclic voltammetry while compound $\mathbf{10}_9$ with a fourth oxidation step shows reversible electron-transfer reactions. This clearly demonstrates that highly charged species can be stabilized in extended conjugated π-systems.

The plots of the oxidation potentials vs the reciprocal number *n* of thiophene units of the oligothiophenes $\mathbf{10}_n$ give an unexpected and up until now unknown increase of the first oxidation step while the higher electron-transfer steps decrease in their potentials with growing *n*. The latter behavior is known for other oligothiophene series, such as in the series of α,α′-bis(diphenyl)-capped oligothiophenes,[23] α,α′-bis(ditolylaminophenyl)-capped oligothiophenes,[24] oligothiophenes end-capped by bis(cyclohexeno) units,[25] or oligothiophenes with bicyclo[2.2.2]octane frameworks.[26] The first electron transfer differs in its dependence of the oxidation potentials on the number of thiophene units *r* from that of the series of α-diphenylamino-capped oligothiophenes $\mathbf{8}_r$. Here, the first oxidation potential decreases, as expected, with growing *r*.

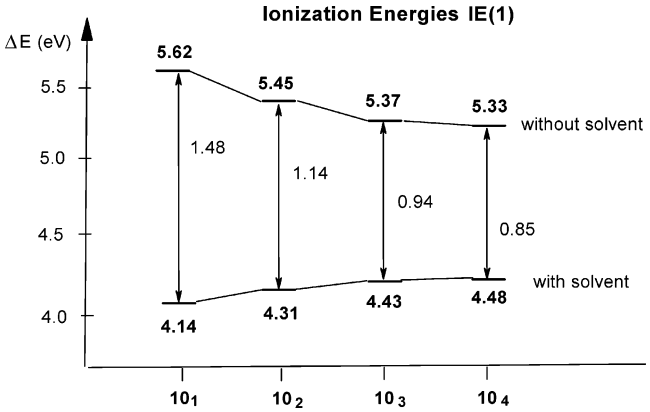

Figure 3. First ionization energies of neutral α,α′-bis(diphenylamino)-capped oligothiophenes $\mathbf{10}_n$ with and without consideration of the solvent effect by IPCM (acetonitrile) in electronvolts (B3LYP/3-21G optimum geometries).

Ionization energies ("ionization potentials") of the oligothiophenes may be used to understand the unexpected chain length dependencies of the first oxidation potential. Unfortunately, due to the low volatility of the compound studied, the gas phase ionization potentials (IE_1) are not available by electron spectroscopy. Therefore, these energies are to be calculated by quantum chemical methods. Very recently, the ionization potentials of some α,α′-bis(diphenylamino)-capped oligothiophenes $\mathbf{10}_n$ with $n = 1-4$ at gold surfaces have been estimated.[27] The IE_1 value is defined by the difference in energy of the geometry-optimized ground and the ionized structures (adiabatic ionization energy). According to DFT calculations, the ionization energy of the free molecules decreases in the gas phase from 5.62 eV for monothiophene $\mathbf{10}_1$ to 5.26 eV for hexakisthiophene $\mathbf{10}_6$ (see Figure 3). However, the behavior is different in solution as shown by self-consistent reaction field calculations (IPCM model[18]) with acetonitrile as the solvent. Because larger-sized cations are less stable in acetonitrile than the smaller ones, the stabilizing effect of polar solvents for cations is decreasing with increasing oligomer chain length. Therefore, the decrease of the first ionization energy known

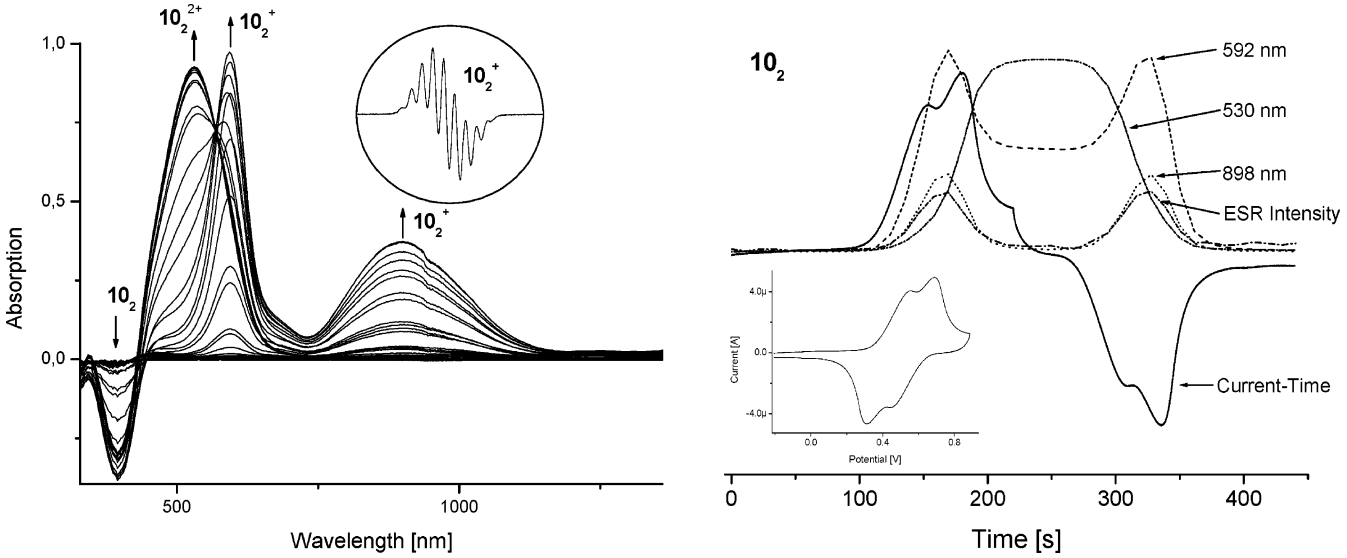

Figure 4. (a) UV−vis/NIR difference spectra of compound $\mathbf{10}_2$ during oxidation scans. (b) Absorption and ESR intensity vs time during the electrochemical oxidation (inset: cyclic voltammogram of the compound under spectroelectrochemical study).

for gaseous molecules is overcompensated by the stabilization of the cation in the solvent. Thus, the ionization energy increases with the chain length (see Figure 2). This may illustrate the unexpected dependence of the first oxidation potentials on chain length found experimentally.

As the first oxidation step changes at $n = 3$ from a single-electron to a two-electron transfer, a change in the chain length dependence of the oxidation potential occurs at this point (see Figure 2). All lines of the oxidation potentials intersect at $1/n = 0.1$ ($n = 10$) implying that for $\mathbf{10}_{10}$ the four-electron transfers are of the same energy resulting in a four-electron-transfer step.

The higher homologues $\mathbf{10}_3-\mathbf{10}_9$ of the α,α'-bis(diphenylamino)-capped oligothiophene series give at higher potentials the dicationic species $\mathbf{10}_3^{2+}-\mathbf{10}_9^{2+}$. At much higher potentials, these dications $\mathbf{10}_5^{2+}-\mathbf{10}_9^{2+}$ can be further oxidized to form stable triple-charged radical cations $\mathbf{10}_5^{3+\bullet}-\mathbf{10}_9^{3+\bullet}$. Furthermore, compounds $\mathbf{10}_6-\mathbf{10}_9$ can be transformed into 4-fold and even into 5-fold oxidized species but only for $\mathbf{10}_9$ is the fourth oxidation step found to be reversible.

In the α-diphenylamino-substituted oligothiophene series $\mathbf{8}_r$, the first oxidation potential decreases, as expected, with an increasing number *n* of thiophene moieties. For $\mathbf{8}_1$ and $\mathbf{8}_2$, cyclic voltammetry gives upon repeated cycling new redox peaks at lower electrode potentials. These peaks are attributed to the corresponding α,α'-bis(diphenylamino)-capped oligothiophenes $\mathbf{10}_2$ and $\mathbf{10}_4$ which are generated during cycling. Obviously, $\mathbf{8}_1$ and $\mathbf{8}_2$ are electrochemically transferred into their dimers $\mathbf{10}_2$ and $\mathbf{10}_4$ by oxidation.[28] In contrast, the higher homologues $\mathbf{8}_3$, $\mathbf{8}_4$, and $\mathbf{8}_5$ are—in accordance with the number of electrons exchanged—transferred into stabilized radical monocations $\mathbf{8}_3^{+\bullet}$, $\mathbf{8}_4^{+\bullet}$, and $\mathbf{8}_5^{+\bullet}$.

Analogous to the compounds $\mathbf{10}_n$, the compounds $\mathbf{8}_3-\mathbf{8}_5$ yield by oxidation rather stabilized radical cations which do not have any remarkable tendency for disproportionation or dimerization. Using the difference of the first and second oxidation potential for the radicals $\mathbf{8}_4^{+\bullet}$ and $\mathbf{8}_5^{+\bullet}$ as well as for the radicals $\mathbf{10}_1^{+\bullet}$ and $\mathbf{10}_2^{+\bullet}$, their stability constants K_s are calculated to be 7.8×10^3, 3.9×10^2, 1.1×10^7, and 1.3×10^2, respectively, applying the known procedure.[29] These values point to a considerable stability of these radicals for disproportion. Unfortunately, the stability constants for the other stabilized mono- and dication radicals cannot be calculated because the difference between their first and second oxidation potentials is too small or their electrode reactions are irreversible.

Hyperfine Splitting Constants

Radical ions can be detected by both their UV−vis absorptions (see Figure 4) as well as their ESR spectra. Thus, for radical cation $\mathbf{10}_1^{+\bullet}$, which exhibits intense absorption maxima at about 470 and 640 nm in the visible range, an ESR spectrum splitted into 7 lines is recorded. For each further homologue of the series $\mathbf{10}_n^{+\bullet}$, two additional lines appear in the ESR spectrum. Thus, for radical cations $\mathbf{10}_2^{+\bullet}$, $\mathbf{10}_3^{+\bullet}$, and $\mathbf{10}_4^{+\bullet}$, 9, 11, and 13 lines, respectively, were recorded. The splitting of these lines decreases by increasing the number *n* of thiophene moieties in the oligomer. As a consequence, no hyperfine splitting is observed for the radical cations of the higher homologues, namely, for species $\mathbf{10}_5^{+\bullet}-\mathbf{10}_9^{+\bullet}$. This is illustrated in Figure 5.

The increase in the number of ESR lines and the decrease in the splitting constant with increasing thiophene units *n* suggest that the unpaired electron in the cation radicals is mainly delocalized on the oligothiophene units including the adjacent amino groups. Thus, only the C−H coupling of the β-positions and the C−N coupling of the α-position are detectable in the ESR spectra. The β-carbon atoms in the substituted oligothiophene units have identical spin densities in each compound. The spin density in the phenyl groups of the end caps is very low, and therefore, no influence of these groups on the ESR hyperfine structure can be detected.

As compounds $\mathbf{10}_3-\mathbf{10}_9$ give two-electron transfers in their first oxidation steps, no primary radicals are formed in this step. Nevertheless, an ESR signal is recorded at this step as radicals are formed by a synproportion reaction of the corresponding parent compound and its doubly oxidized species. Using the difference between the electrode potentials of the first two one-electron transfers, the radical cation formation constant by synproportionation K_s can be estimated as given before. Because the K_s values decrease with increasing chain length, the stability of the radical cations of the higher homologues decreases significantly. Thus, the radical cations of compounds $\mathbf{10}_8$ and $\mathbf{10}_9$ are formed at such low concentrations that they are undetectable by ESR measurements.

As given for compound $\mathbf{10}_2$ (Figure 4b), an increase of the ESR signal is detected at the first oxidation step at −0.010 V

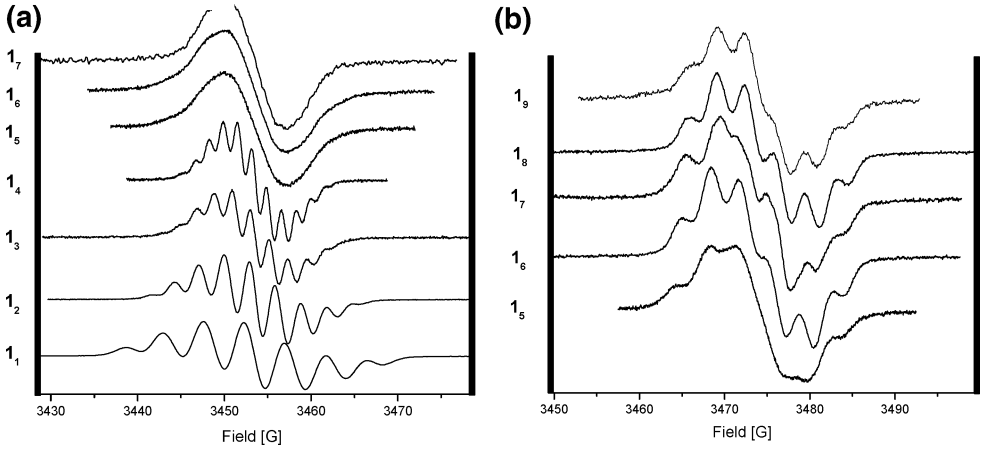

Figure 5. ESR spectra of the electrochemical produced radical cations (a) and the radical trications (b) of the series of α,α′-bis(diphenylamino)-capped oligothiophenes $\mathbf{10}_n$ (the spectra are shifted for clarity).

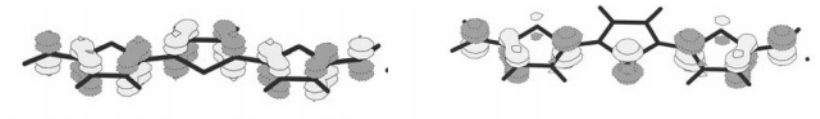

Figure 6. Shape of the singly occupied Kohn−Sham orbitals of the α,α′-bisamino-substituted tristhiophene radical mono- and trications $\mathbf{13}_n^{+\bullet}$ (part a, a_2 symmetry) and $\mathbf{13}_n^{3+\bullet}$ (part b, b_1 symmetry).

accompanied by two new absorptions in the UV−vis spectrum at 592 and 898 nm. This is caused by the radical monocation $\mathbf{10}_2^{+\bullet}$. In the next electron-transfer step at +0.115 V, the ESR signal intensity as well as the absorptions at 592 and 898 nm disappear. Simultaneously, a new intense absorption band with a maximum at 530 nm is observed and can be attributed to the dicationic species $\mathbf{10}_2^{2+}$.

A similar behavior is found for the higher homologues of $\mathbf{10}_n$ which can be transformed electrochemically into their dicationic species $\mathbf{10}_n^{2+}$. Compound $\mathbf{10}_5$ and its higher homologues $\mathbf{10}_6$−$\mathbf{10}_9$ give ESR signals at higher electrode potentials attributed to radical trications $\mathbf{10}_n^{3+\bullet}$. By shorter-chain compounds, these ESR signals are overlapped by those of the radical monocations $\mathbf{10}_n^{+\bullet}$ which are formed simultaneously.

The ESR spectra of the tricationic radicals $\mathbf{10}_n^{3+\bullet}$ consist of broad lines (see Figure 5b). The *g*-factor of the radical monocations is in the range of 2.0025, while that of the radical trications is around 2.0035. The larger *g*-factor of the latter is caused by a stronger localization of the unpaired electron at the sulfur atoms in the thiophene moieties.

These experimental results can be explained by the calculated spin density distribution. As exemplified in Figure 6, the π-type SOMOs of the radical monocation $\mathbf{13}_3^{+\bullet}$ and trication $\mathbf{13}_3^{3+\bullet}$ are highly delocalized. The SOMO of the radical monocation $\mathbf{13}_3^{+\bullet}$ is antisymmetric with respect to the plane perpendicular to the molecular plane while the SOMO of the radical trication $\mathbf{13}_3^{3+\bullet}$ is symmetric. As a consequence, the sulfur atoms of the trication show a remarkably high spin density contrary to those of the monocation. Therefore, the *g*-factor is larger for trications than for monocations. Isotropic Fermi contact couplings between the magnetic moments of the nitrogen as well as hydrogen nuclei and the unpaired electrons were calculated at the B3LYP/6-31G* level of theory. The calculated hyperfine splitting constants of the monocations $\mathbf{13}_n^{+\bullet}$ and trication $\mathbf{13}_n^{3+\bullet}$ are given together with the experimental data in Table 2.

Whereas the sign of hyperfine splitting (hfs) constants cannot be determined experimentally, theoretical calculations give a clear indication whether they are either positive or negative.

TABLE 2: ESR Data of Electrochemically Generated Oxidation Products of α,α′-Bis(diphenylamino)-capped Oligothiophenes $\mathbf{10}_n$

	calcd[a]					exp[b]		
		a						
entry	a_N	α	*β*	*γ*	*δ*	a_{phen}	a_N	a_H*
$\mathbf{10_1}^+$	4.9	−3.6				−0.8 − 0.6	4.6	4.0
$\mathbf{10_2}^+$	3.3	−2.5	−2.5			−0.5 − 0.4	2.9	2.7
$\mathbf{10_3}^+$	2.4	−1.7	−2.2	−1.9		−0.4 − 0.3	2.2	2.0
$\mathbf{10_4}^+$	1.9	−1.3	−2.0	−1.3	1.8	−0.3 − 0.3	2.0	1.7
$\mathbf{10_1}^{3+\bullet}$	1.5	−0.3				−2.8 − 0.8		
$\mathbf{10_2}^{3+\bullet}$	3.2	−1.8	1.6			−2.6 − 0.8		
$\mathbf{10_3}^{3+\bullet}$	4.1	−3.2	2.6	0.1		−2.3 − 0.7		
$\mathbf{10_4}^{3+\bullet}$	4.5	−4.1	2.8	−1.7	1.8	−1.7 − 0.6		

[a] The hfs of $\mathbf{10_2}$ calculated with 6-31G* and 6-311G* optimum geometries with the same functionals $a_N = 3.2$, $a_{H\alpha} = 2.5$, $a_{H\beta} = 2.4$ and $a_N = 3.8$, $a_{H\alpha} = 2.1$, $a_{H\beta} = 2.1$, respectively (see text). [b] Splitting of the hydrogens not resolved.

The hfs constants a_H show a regular shift, and their absolute values of both cation radicals vary moderately along the hydrocarbon chain. They decrease with the number of thiophene rings. Whereas the a_N values of monocations decrease in this sequence, the a_N values of the trications increase. The change of the theoretical and experimental hfs values and the numerical values are in satisfactory agreement. The deviation of theoretical values from experimental ones is expected to be in the range of 10−15% as reported in the literature.[13] An improvement of the level of theoretical calculations by geometry optimization with a larger Gaussian split double-ζ or triplet-ζ valence basis set including geometry optimizations did not improve the correspondence (see footnote of Table 2). Gaussian-type basis sets do not adequately consider the dependence of isotropic coupling on the spin density at different nuclear positions. As no experimental hfs constants could be recorded for the radical trications, conclusions can only be drawn from theoretical considerations. The calculations suggest a more complex hfs, and the calculated a_H values vary siginificantly along the hydrocarbon chain.

TABLE 3: Experimental and Calculated Absorption Wavelength of α,α′-Diamino-capped Oligothiophenes 13_n at Different Steps of Oxidation

	10_n					10_n^{2+}					$10_n^{+\bullet}$				
		theory					theory					theory			
	experiment	TD-DFT[a]		PPP		experiment	TD-DFT[a]		PPP		experiment	TD-DFT[a]			
	(nm)	(nm)	(lg ε)	(nm)	(lg ε)	(nm)	(nm)	(lg ε)	(nm)	(lg ε)	(nm)	(nm)	(lg ε)	(nm)	(lg ε)
1	310	360	(0.31)	305	(0.71)	502	666	(0.45)	809	(1.07)	470	423	(0.17)	665	(0.27)
2	396	455	(0.74)	365	(1.34)	530	684	(1.01)	778	(1.70)	643	538	(1.34)	843	(0.29)
3	432	482	(1.25)	411	(1.84)	650	716	(1.73)	822	(2.67)	592	632	(1.53)	1076	(0.32)
4	445	526	(1.73)	443	(2.23)	816	780	(2.47)	925	(3.64)	898	718	(1.94)	1315	(0.43)
5	471	568	(2.25)	473	(2.67)	995	863	(3.16)	1053	(4.58)	718	795	(2.21)	1554	(0.59)
6	486	600	(2.65)	498	(3.12)	1201	963	(3.78)	1323	(5.66)	1300	862	(2.33)	1791	(0.79)

[a] B3-LYP/3-21G model.

UV−vis/NIR Spectral Absorptions

To characterize the products formed by electrochemical oxidation of α,α′-bis(diphenylamino)-substituted oligothiophenes $\mathbf{10}_n$, in situ spectroelectrochemical measurements of the optical and ESR spectra at a laminated gold-LIGA electrode in a thin layer cell (1 mm thickness)[28] were performed (Table 2). An example is given for $\mathbf{10}_2$ in Figure 4.

All oxidized species were detected by their long-wave absorption in the UV−vis/NIR region. Absorptions occur in voltammetric forward scans which disappear completely in the back scan. The absorption bands of the monocationic species seem to exist even at the end of the forward scan only in some cases, because of the band overlap with a new absorption originating from the dicationic species. For example, the absorption band at 592 nm for the monocationic species $\mathbf{10}_2^{+\bullet}$ is not completely vanished due to the overlap between the band at 530 nm for the dicationic species $\mathbf{10}_2^{2+}$ (see Figure 4).

For a better understanding of the chromophoric properties and the nature of the lowest-energy electronic excitation, the neutral compounds $\mathbf{10}_n$ and dicationic compounds $\mathbf{10}_n^{2+}$ of the α,α′-bis(diphenylamino)-substituted oligothiophene series were calculated by the TD-DFT method. Because the electronic transistions of interest are of the $\pi \rightarrow \pi^*$-type, the semiempirical Pariser−Parr−Pople (PPP) method was also applied using the formerly derived parameters without any additional arbitrary assumptions. Experimental and calculated spectral data are listed in Table 3. Calculated PPP data of the $\pi \rightarrow \pi^*$ transitions of a large series of middle-sized sulfur-containing compounds agreed satisfactorily well with the experimental data at an average absolute deviation of 0.20 eV. This deviation is comparable with that obtained by first-principle methods such as TD-DFT (0.21 ev). In the case of neutral oligothiophenes $\mathbf{10}_n$, the error of transition energies is, however, nearly twice as large. The transition energy errors are reduced from 0.44 to 0.27 eV when the 3-21G basis set is replaced by the 6-31G* basis and will be additionally lowered when adiabatic rather than vertical S/T energy gaps are considered. Thus, cationic oligothiophenes deserve interest not only because of the unique electronic structure but also with respect to the energetic characteristics. In contrast to TD-DFT calculations, the semiempirical PPP procedure reproduces the experimental data of the neutral compounds very well. The situation is more complex in the case of the 2-fold charged species $\mathbf{10}_n^{2+}$. For longer-chain compounds, the deviation of the theoretical absorption wavelength from the experimental ones is at least at an acceptable range.

The absorption wavelengths of the neutral oligothiophenes $\mathbf{10}_n$ undergo a steady red shift with the extension of chain length. As is known for polyacetylene, the absorption wavelength may reach convergence at a limiting value of about 2 eV (620 nm). The calculated absorption intensities of the neutral compounds are relatively low. The lowest energy transitions of the neutral compounds as well as those of the dications are essentially of the highest occupied molecular orbital−lowest unoccupied molecular orbital (HOMO−LUMO) type, and the transitions are polarized along the longest molecular axis. Since the LUMO of the dications $\mathbf{10}_n^{2+}$ is considerably lower in energy than that of the neutral compounds, the absorption bands are shifted into the NIR region. In contrast to neutral compounds, the shift increases with each inserted thiophene unit in the dications. As indicated by the oscillator strength, the absorption intensities simultaneously increase strongly. The high absorption intensity of $\mathbf{10}_6^{2+}$ is reminiscent of long-chain polymethine dyes. The intensity is on the same order of magnitude as that of bis(4-dipyrido)icosipentamethine, a polymethine dye with 25 methine groups, as calculated by the same approximation.

According to the quantum chemical calculations, the long-wavelength spectrum of the π-type radical $\mathbf{10}_n^{+\bullet}$ is determined by two electronic transitions that essentially arise from HOMO−SOMO and SOMO−LUMO one-electron transitions. The higher energy component exhibits the larger intensity. Since the theoretical calculations of open-shell systems are spin-contaminated in the UDFT approximation, the numerical data may be affected but not the general conclusions. Because the theory predicts a regular shift of the absorption bands with increasing chain lengths of $\mathbf{10}_n^{+\bullet}$, the inconsistency in the experimental data of Table 3 needs to be explained. Attention has to be paid to the theoretical prediction that two long-wavelength absorption bands occur.

The calculations of spectral data were likewise performed for the parent structures **13** with an extended basis taking into account additionally a set of polarization and diffuse functions. Selected results are reported in Table 4 for the open-shell monocations $\mathbf{13}_n^{+\bullet}$ and trications $\mathbf{13}_n^{3+\bullet}$. The planar molecules are of higher symmetry than the related tetraphenyl-substituted compounds of the series $\mathbf{10}_n$. Molecules of series **13** belong to either the point group C_{2h} or C_{2v} giving rise to $A_g \rightarrow B_u$ and $A_g \rightarrow A_g$ transitions, respectively.

As mentioned above, there are two transitions of the same symmetry ($A_g \rightarrow B_u$) that dominantly contribute to the long-wavelength absorptions. Forbidden $A_g \rightarrow A_g$ transitions may be available. Remarkably, the calculated wavelengths of the two lowest-energy transitions of the mono- and trication radicals are very similar.

Molecular and Electronic Structure

All details of the structure of the homologous α,α′-bis-(phenylamino)-capped oligothiophenes $\mathbf{10}_n$ and the related mono- and dications are summarized here, and more general conclusions on the nature of these compounds are to be made.

TABLE 4: Absorption Wavelength and Oscillator Strength of Radical Cations Derived from α,α′-Diamino-capped Oligothiophenes 13_n Calculated by TD-UDFT in Two Approximations[a]

	B3LYP/3-21G								B3LYP/3-21+G*							
n	$13_n^{+\bullet}$		$13_n^{3+\bullet}$						$13_n^{+\bullet}$		$13_n^{3+\bullet}$					
1	288	(0.33)	393	(0.02)	245	(0.33)			304	(0.33)	399	(0.01)	247	(0.34)	564	(<0.01)
2	413	(0.72)	641	(0.03)	354	(0.60)			434	(0.74)	652	(0.02)	436	(0.23)	632	(0.01)
3	520	(1.55)	883	(0.07)	500	(0.82)	864	(0.01)	544	(1.16)	897	(0.06)	508	(0.78)	871	(0.01)
4	614	(1.62)	1112	(0.14)	527	(0.92)	1097	(0.02)	641	(1.57)	1130	(0.13)	644	(0.86)	1108	(0.02)
5	700	(1.97)	1329	(0.25)	697	(2.12)	1325	(0.03)	728	(1.92	1351	(0.24)	713	(2.12)	1346	(0.03)
6	778	(2.21)	1539	(0.40)[b]	789	(2.71)	1532	(0.05)	806	(2.16)	1564	(0.39)	807	(2.67)	1562	(0.05)

[a] TD-DFT calculation based on B3LYP/3-21G. [b] Geometries calculations with optimized B3LYP/3-21+G* geometries of $\mathbf{13_4}$ radicals resulted in 641 nm (lg ϵ, 1.57) and 1130 nm (lg ϵ, 0.13) for the monocation and 616 nm (lg ϵ, 1.19) and 1125 nm (lg ϵ, 0.03) for the trication.

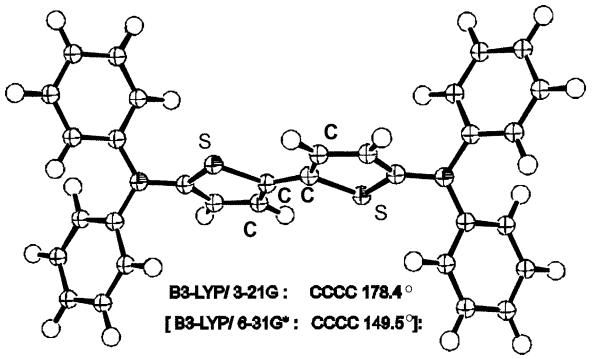

Figure 7. Structure of the 5,5′-bis(diphenylamino)-2,2′-bithiophene $\mathbf{10_2}$ according to DFT calculations. The thienyl groups are nearly coplanar at the B3LYP/3-21G level of theory while twisting occurs with a more extended basis set such as B3LYP/6-31G*.

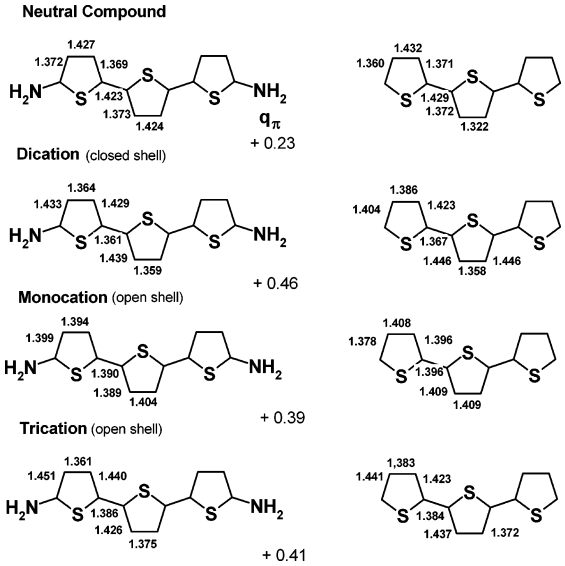

Figure 8. Selected bond lengths in angstroms along the hydrocarbon backbone of the α,α′-bisamino-substituted tristhiophene $\mathbf{13_3}$ calculated as a neutral, monocationic, dicationic, and tricationic compound. The positive numbers are calculated π-charges of the terminal nitrogen corresponding to formal charges.

When the procedures of this work are taken into account, the chemical structures were optimized in the energetically favored transoid conformation. As mentioned above, the terminal phenyl and the amino groups are more or less strongly twisted out of the molecular plane. (This is demonstrated in Figure 7 for the neutral 5,5′-bis(diphenylamino)-2,2-bithiophens $\mathbf{10_2}$.) At the B3LYP/3-21G level, the oligothiophene substructure of the series $\mathbf{10}_n$ is planar. However, a planar oligothiophene structure conflicts with experimental results on amino-group-free parent compounds.[30] If the 3-21G basis set is replaced by the more extended 6-31G* basis set, then the thiophene rings of 5,5′-bis(diphenylamino)-2,2-bithiophene $\mathbf{10_2}$ are twisted around the inter-ring CC-bond. The CCCC dihedral angle of the two thiophene groups amounts to 158°. Moreover, the amino groups are pyramidal by 133.5° rather than planar. This DFT result corresponds with the result of the MP2/6-31G* ab initio calculation resulting in an angle of distortion of 145.3° and an angle of pyramidalization of 130.1°. However, calculations have shown that some distortion out of plane does not seriously affect the calculated molecular properties of the oligothiophenes. Therefore, DFT calculations were generally based on 3-21G geometries with planar oligothiophene structures.

The bond length characteristics of α,α′-diamino-capped tristhiophene $\mathbf{13_3}$ and of their cations are given in Figure 8 including the corresponding bond lengths of the parent tristhiophenes. The neutral and dicationic closed-shell oligothiophenes $\mathbf{13_3}$ and $\mathbf{13_3}^{2+}$ display polyenic structures with alternating single and double bonds. This bond structure is well reflected with the formulas of Scheme 3. The cation radical $\mathbf{13_3}^{+\bullet}$ cannot be attributed to a singular structural formula since the CC bonds are almost the same. The radical $\mathbf{13_3}^{+\bullet}$ as a monocation is between the neutral compound **13** and its dicationic species $\mathbf{13_3}^{2+-}$. The bond delocalization of the radical is less pronounced for the unsubstituted tristhiophene (see Figure 8).

The situation of the cation radicals $\mathbf{13}_n^{+\bullet}$ remind us of the α,α′-diamino-substituted streptopolymethine radical dyes investigated in a previous study.[31] The structure of the cation radicals $\mathbf{13}_n^{+\bullet}$ differs from that of the chain-type polymethine radicals by the sulfur bridges that imply oligothiophene structural rigidity. The terminal amino groups have a pronounced donor effect. Bond equalization is not observed with the trication radicals $\mathbf{13}_n^{3+\bullet}$ (see Figure 8 for $n = 3$).

Cations and dications are termed polarons and bipolarons in condensed matter physics terminology.[32] As charge carriers, they are essential for the electric conductivity of organic materials. The question arises whether charged states at longer-chain compounds are more adequately described as polaron pairs with charge separation than as bipolarons, that is, whether two polarons may be stable in a single molecule rather than a bipolaron. Recent experimental results on parent oligothiophenes favored such a structure provided that the number *n* of thiophene groups of the parent oligothiophene dications is sufficiently large, for example, $n = 6$[30] or $n = 12$.[33]

According to UB3LYP calculations of $\mathbf{10}_n^{2+}$ using the 3-21G basis set, the bipolaron is the stable dicationic structure for oligomers up to the tetrathiophene $\mathbf{10_4}^{2+}$. Beyond this threshold, bipolarons are instable. UDFT calculations of pentathiophene dication $\mathbf{10_5}^{2+}$ and the higher members of this homologous series induce broken symmetry (BS) solutions that are lower in energy than those of the conventional spin-restricted (RDFT) approach. As shown by RDFT calculations using the 3-21G basis set as

SCHEME 3

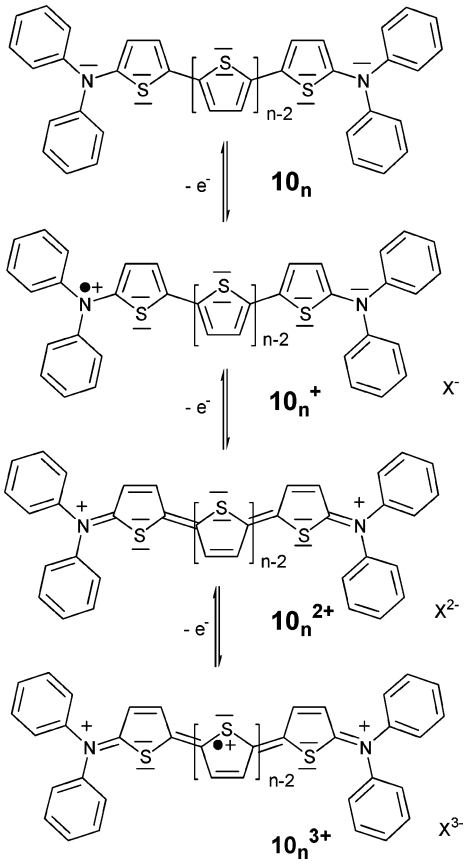

summarized in Figure 9, the depression energy increases with the chain length. This stabilization energy of the pentathiophene dication $\mathbf{10}_5^{2+}$ amounts to 0.01 eV (0.23 kcal/mol) but increases to −0.06 eV when the basis set 3-21G is replaced by 6-31G*. The weakness in the conventional description of oligothiophene dications as closed-shell structures was first reported by semiempirical calculations of the parent oligothiophenes employing a four-reference wave function[34] and was later substantiated by UDFT calculations for these compounds.[35] Vertical singlet−triplet splitting energies are also mentioned in Figure 9. The triplet energies approach the corresponding singlet energies with increasing chain lengths. The S/T energy of $\mathbf{10}_5^{2+}$ is reduced from 0.44 to 0.27 eV when the 3-21G basis set is replaced by the 6-31G* basis in the calculations and will be additionally lowered when adiabatic rather than vertical S/T energy gaps are considered. Thus, cationic oligothiophenes seem to make the existence of the polaron pair possible. Therefore, they deserve interest because of the unique electronic structure of their energetic characteristics.

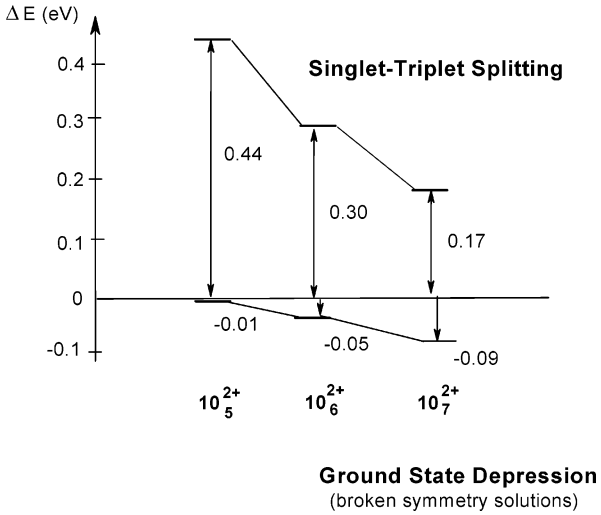

Figure 9. Singlet−triplet splitting and ground-state depression energies in electronvolts of α,α′-bis(diphenylamino)-capped oligothiophene dications $\mathbf{10}_n^{2+}$ (see text).

Conclusions

α,α'-bis(diphenylamino)-substituted oligothiophenes $\mathbf{10}_n$ as a new series of end-capped oligothiophenes were synthesized by a palladium-catalyzed C,C-coupling reaction of stannylated 2-diphenylaminothiophenes and their thiophene homologues with 2,5-dibromothiophene and its homologues. The new compounds are to be easily oxidized electrochemically giving stabilized monocation radicals $\mathbf{10}_n^{+\bullet}$, dications $\mathbf{10}_n^{2+}$, and in the case of higher homologues, 3-fold, 4-fold, and 5-fold oxidized species $\mathbf{10}_n^{\mu+}$ ($\mu = 3$, 4, or 5). The electrochemical oxidation was studied by cyclic voltammetry and in situ ESR/UV−vis/NIR spectroscopy. The oxidation potentials were found to show an unknown dependency on the inverse number *n* of thiophene units. The slope of the first one-electron oxidation potentials was different from that of higher oxidation steps. It could be explained by a solvent effect. Thus, small radical monocations are stabilized by a stronger polar solvent than larger radical monocations. In contrast to the neutral oligothiophenes $\mathbf{10}_n$, the UV−vis absorption maxima of the cations are shifted to longer wavelengths with an increasing number *n* of thiophene units.

Restricted and unrestricted DFT calculations were performed to substantiate and to rationalize the results of the spectroelectrochemical studies. The spectral properties of the closed-shell oligothiophenes $\mathbf{10}_n$ and $\mathbf{10}_n^{2+}$ are satisfactorily reproduced by TD-DFT calculations. The long-wave absorption maxima of these compounds were correctly predicted as two band spectra of the open-shell monocations $\mathbf{10}_n^{+\bullet}$ and trications $\mathbf{10}_n^{3+\bullet}$. Neutral and dicationic oligothiophenes $\mathbf{10}_n$ and $\mathbf{10}_n^{2+}$, respectively, are essentially polyenic in nature with mainly alternating CC single and double bonds inside and between the thiophene fragments. However, in the case of the radical monocations $\mathbf{10}_n^{+\bullet}$, the CC-bonds are almost equal, similar to the amino-substituted polymethine structures. Calculations have also revealed that the longest-wavelength absorptions of the long-chain dications $\mathbf{10}_n^{2+}$ are very strong. The dications $\mathbf{10}_n^{2+}$ represent, therefore, a new class of chromophores with intense long-wavelength absorptions. UDFT calculations of $\mathbf{10}_n^{2+}$ have also shown that dications of a sufficient chain length give two-polaron electronic structures.

Acknowledgment. The authors appreciate the Deutsche Forschungsgemeinschaft for financial support and Prof. Dr. R. Gleiter, University of Heidelberg, for trying to measure the ionization potentials of the α,α′-bis(diphenylamino)-capped oligothiophenes $\mathbf{10}_n$ by photoelectron spectroscopy.

References and Notes

(1) (a) Shirota, Y. *J. Mater. Chem.* **2000**, *10*, 1. (b) Fuhrmann, T.; Salbeck, J. *Adv. Photochem.* **2002**, *27*, 83. (c) Strohrigl, P.; Graulevicius, J. V. *Adv. Mater.* **2002**, *14*, 1439.

(2) Horowitz, G. *Adv. Mater.* **1998**, *10*, 365.

(3) (a) Johnson, G. E.; McGrane, K. M.; Stolka, M. *Pure Appl. Chem.* **1995**, *67*, 175. (b) Noda, T.; Ogawa, H.; Noma, N.; Shirota, Y. *J. Mater. Chem.* **1999**, *9*, 2177. (c) Shirota, Y.; Okumoto, K.; Inada, H. *Synth. Met.* **2000**, *111*−*112*, 387.

(4) (a) Sacriciftci, N. S.; Smilowitz, L.; Heeger, A. J.; Wudl, F. *Science* **1992**, *258*, 1474. (b) Halls, J. J. M.; Walsh, C. A.; Greenham, N. C.;

Marseglia, E. A.; Friend, R. H.; Moratti, S. C.; Holmes, A. B. *Nature* (London) **1965**, *376*, 498.

(5) Getautis, V.; Stanisauskaite, A.; Paululis, O.; Uss, S.; Uss, V. *J. Prakt. Chem*. **2000**, *342*, 58.

(6) (a) Yamamoto, T.; Nishiyama, M.; Koie, K. *Tetrahedron Lett*. **1998**, *39*, 617. (b) Schumann, J.; Kanitz, A.; Hartmann, H. *Synthesis* **2002**, 1268. (c) Gerstner, P.; Rohde, D.; Hartmann, H. *Synthesis* **2002**, 2487. (d) Wong, K.-T.; Hung, T. H.; Kao, S., C.; Chou, C. H.; Su, Y. O. *Chem. Commun*. **2001**, 1628.

(7) Hartmann, H.; Gerstner, P.; Rohde, D. *Org. Lett*. **2001**, *3*, 1673.

(8) Tabet, A.; Schröder, A.; Hartmann, H.; Rohde, D.; Dunsch, L. *Org. Lett*. **2003**, *5*, 1817.

(9) (a) Hassan, J.; Sévignon, Marc.; Gozzi, C.; Schultz, E.; Lemaire, M. *Chem. Rev*. **2002**, *102*, 1359. (b) Prim, D.; Campaigne, J.-M.; Joseph, D.; Andrioletti, B. *Tetrahedron* **2002**, *58*, 2041. (c) Hartwig, J. F. *Angew. Chem*. **1998**, *110*, 2155; *Angew. Chem., Int. Ed. Engl*. **1998**, *37*, 2047. (d) Ley, S. V.; Thomas, A. W. *Angew. Chem*. **2003**, *115*, 5558−5607; *Angew. Chem., Int. Ed. Engl*. **2003**, *42*, 5400−5449. (e) Yang, B. H.; Buchwald, S. L. *J. Organomet. Chem*. **1999**, *567* (1−2), 125. (f) Wolfe, J. P.; Wagaw, S.; Marcoux, J.-F.; Buchwald, S. L. *Acc. Chem. Res*. **1998**, *31*, 805.

(10) Tabet, A.; Hartmann, H. *Synthesis* **2005**, 610.

(11) Periasamy, M.; Jayakumar, K. N.; Bharathi, P. *J. Org. Chem*. **2000**, *65*, 3548.

(12) Li, Z. H.; Wong, M. S.; Tao, Y.; D'Iorio, M. *J. Org. Chem*. **2004**, *69*, 921.

(13) Koch, W.; Holthausen, M. C. *A Chemist's Guide for Density Functional Theory*; Wiley-VCH: Weinberg, Germany, 2000.

(14) Frisch, M. J.; Trucks, G. W.; Schlegel, H. B.; Scuseria, G. E.; Robb, M. A.; Cheeseman, J. R.; Zakrzewski, V. G.; Montgomery, J. A., Jr.; Stratmann, R. E.; Burant, J. C.; Dapprich, S.; Millam, J. M.; Daniels, A. D.; Kudin, K. N.; Strain, M. C.; Farkas, O.; Tomasi, J.; Barone, V.; Cossi, M.; Cammi, R.; Mennucci, B.; Pomelli, C.; Adamo, C.; Clifford S.; Ochterski, J.; Petersson, G. A.; Ayala, P. Y.; Cui, Q.; Morokuma, K.; Malick, D. K.; Rabuck, A. D.; Raghavachari, K.; Foresman, J. B.; Cioslowski, J.; Ortiz, J. V.; Stefanov, B. B.; Liu, G.; Liashenko, A.; Piskorz, P.; Komaromi, I.; Gomperts, R.; Martin, R. L.; Fox, D. J.; Keith, T.; Al-Laham, M. A.; Peng, C. Y.; Nanayakkara, A.; Gonzalez, M.; Challacombe, M.; Gill, P. M. W.; Johnson, B.; Chen, W.; Wong, M. W.; Andres, J. L.; Head-Gordon, M.; Replogle, E. S.; Pople, J. A. *GAUSSIAN 98*, revision A.7; Gaussian, Inc.: Pittsburgh, PA, 1998.

(15) Becke, A. D. *J. Chem. Phys*. **1993**, *98*, 1372−1377.

(16) Lee, C.; Yang, W.; Parr, R. G. *Phys. Rev. B* **1988**, *37*, 785−789.

(17) For implementation of B3LYP in GAUSSIAN, see Stephens, P. J.; Devlin, F. J.; Chabalowski, C. F.; Frisch, M. J. *J. Phys. Chem*. **1994**, *98*, 11623−11627.

(18) Foresman, J. B.; Keith, T. A.; Wiberg, K. B.; Snoonian, J.; Frisch M. J. *J. Phys. Chem*, **1996**, *100*, 16098.

(19) Ridley, J.; Zerner, M. *Theor. Chim. Acta* **1973**, *32*, 111−134.

(20) Fabian, J. *Theor. Chem. Acc*. **2001**, *106*, 199−217.

(21) Moschny, T. *Program package WINPPP*; FH Merseburg: Merseburg, Germany, 1995.

(22) Schaftenaar, G. *MOLDEN*, release 3.5; Nijmegen, The Netherlands, 1999.

(23) Apperloo, J. J.; Groenendaal, L. B.; Verheyen, H.; Jayakanna, M.; Janssen, R. A. J.; Dkhissi, A.; Beljonne, D.; Lazzaroni, R.; Brédas, J.-L. *Chem.−Eur. J*. **2002**, *8*, 2384.

(24) Noda, T.; Ogawa, H.; Noma, N.; Shirota, Y. *J. Mater. Chem*. **1999**, *9*, 2177.

(25) Bäuerle, P.; Segelbacher, U.; Maier, A.; Mehring, M. *J. Am. Chem. Soc*. **1993**, *115*, 10217.

(26) Wakamiya, A.; Yamazaki, D.; Nishinaga, T.; Kitagawa, T.; Komatsu, K. *J. Org. Chem*. **2003**, *68*, 8305.

(27) Liu, X.; Knupfer, M.; Dunsch, L.; Tabet, A.; Hartmann, H. *Org. Electron*. **2006**, *7*, 107−113.

(28) Rapta, P.; Zeika, O.; Rohde, D.; Hartmann, H.; Dunsch, L. *ChemPhysChem* **2006**, in press.

(29) (a) Hünig, S.; Berneth, H. *Top. Curr. Chem*. **1980**, *92*, 1. (b) Èsarsky, P.; Hünig, S.; Scheutzow, D.; Zahradník, R. *Tetrahedron* **1969**, *25*, 4781.

(30) Lane, P. A.; Liess, M.; Vardeny, Z. V.; Partee, J.; Uhlhorn, B.; Shinar, J.; Ibrahim, M.; Frank, A. J. *Proc. SPIE Int. Soc. Opt. Eng*. **1997**, *3145*, 475−482.

(31) (a) Fabian, J.; Hartmann, H. *J. Mol. Struct*. **1975**, *27*, 67−78. (b) Fabian, J.; Hartmann, H. *Theor. Chim. Acta* **1975**, *36*, 351−358.

(32) (a) Cremer, D. *Mol. Phys*. **2002**. *98*, 1899−1940. (b) Gräfenstein, J.; Kraka, E.; Filatov, M.; Cremer, D. *Int. J. Mol. Sci*. **2002**, *3*, 360−364. (c) Cremer, D.; Filatov, M.; Polo, V.; Kraka, E.; Shaik, S. *Int. J. Mol. Sci*. **2002**, *3*, 604−638. (d) Gräfenstein, J.; Hjarpe, A. M.; Kraka, E.; Cremer, D. *J. Phys. Chem*. **2000**, *104*, 1748−1761.

(33) Van Haare, J. A. E.; Havinga, E. E.; van Dongen, J. L. J.; Janssen, A. J.; Cornil, J.; Brèdas, J.-L. *Chem.−Eur. J*. **1998**, *4*, 1509−1522.

(34) Tol, A. J. W. *Chem. Phys*. **1996**, *208*, 73−79.

(35) Gao, Y.; Liu, Ch-G.; Jiang, Y.-S. J. *Phys. Chem*. **2002**, *106*, 5380−5384.